Polymer Bulletin 57, 575–586 (2006)
DOI 10.1007/s00289-006-0572-9

Polymer Bulletin

The influence of fatty acid coating on the rheological and mechanical properties of thermoplastic polyurethane (TPU)/nano-sized precipitated calcium carbonate (NPCC) composites

L. Jiang[1], Y. C. Lam[2] (✉), K. C. Tam[2], D. T. Li[2], J. Zhang[1]

[1] Wood Materials and Engineering Laboratory, Washington State University, Pullman, WA 99164-1806
[2] School of Mechanical and Aerospace Engineering, Nanyang Technological University, 50 Nanyang Avenue, Singapore 639798, Republic of Singapore

E-mail: myclam@ntu.edu.sg, Fax: +65-6791 1859

Received: 3 March 2006 / Revised version: 6 April 2006 / Accepted: 18 April 2006
Published online: 17 May 2006 – © Springer-Verlag 2006

Summary

TPU was reinforced by two types of NPCC particulates (NPCC201 and 401) through melt compounding. Thermal analysis suggested that all the stearic acid coating on NPCC201 was attached to the particulate surface by forming calcium stearate, whereas the fatty acid coating of NPCC401 was excessive and part of the coating existed as free fatty acids. The tensile modulus of TPU/NPCC composites increased slightly with the addition of NPCC, while the toughness showed a larger increase. TPU/NPCC401 showed a unique rheological behavior which has not been reported before. In dynamic shear, G' increased with particulate loading at low frequencies but decreased at high frequencies. In steady shear, viscosity decreased with NPCC loading and an additional Newtonian plateau was observed at low shear rates. The free fatty acid coating on NPCC401 surface was believed to dissipate into the TPU matrix and generate this unique behavior. These results show the importance of achieving optimal coating. Full coverage of the particulate surface is required to achieve optimal coating effects, but over-coating should be prevented to avoid the deterioration of properties.

Introduction

Polyurethanes constitute a group of polymers with highly versatile properties and a wide range of commercial applications. Polyurethane can be made into fiber, film, soft or rigid foam and other cast or injection-molded products. Matching its huge consumption, polyurethane has been an active research area for years. Significant amounts of research results have been published regarding the synthesis, processing, property tailoring and applications of polyurethane.

Polymers are filled with particles to improve their stiffness and toughness, enhance their barrier properties, boost their resistance to fire and ignition or simply to reduce

cost. The disadvantages of particulate filling include brittleness, opacity, poor processability etc. Nanocomposites, particle-filled polymers for which at least one dimension of the dispersed particles is in the nanometer range, provide a potential solution to these inherent drawbacks of filled polymers. When the nanometer-size particles are dispersed, nanocomposites exhibit markedly improved mechanical, thermal, optical and physico-chemical properties when compared to the pure polymer or conventional (microscale) composites, as first demonstrated by Kojima and coworkers for nylon/clay nanocomposites [1-4]. Improvements include increased moduli, strength and heat resistance, and decreased gas permeability and flammability.

Tien et al synthesized montmorillonite/polyurethane nanocomposites [5]. They found that hydrogen bonding in the hard segments of polyurethane decreased with increasing amounts of montmorillonite regardless of the hard segment ratios. The maximum strength and elongation at break of polyurethane nanocomposites increased dramatically when compared to pristine polyurethane, with the maximum values occurring at 1 wt% montmorillonite concentration. Tien et al also found that the glass transition temperature of the hard segment phase and the storage modulus of segmented polyurethane increased substantially in the presence of a small amount of tethered nano-sized layered silicates from montmorillonite [6]. Furthermore, the heat resistance and degradation kinetics of these montmorillonite/polyurethane nanocomposites were enhanced: a 40 ^{o}C increase in the degradation temperature and a 14% increase in the degradation activation energy occurred in polyurethane containing 1 wt % trihydroxyl swelling agent-modified montmorillonite compared to that of the pristine polyurethane.

Tortora et al [7] also synthesized composites of a polyurethane with an organically modified montmorillonite, covering a wide range of inorganic composition up to 40 wt%. Exfoliation was confirmed by X-ray diffraction. The elastic modulus and yield stress increased with the increase of clay content, but the stress and strain at break showed opposite trend. Sorption did not drastically change on increasing the clay content. Permeability, however, showed a remarkable decrease up to 20% of clay and leveled off thereafter.

Finnigan et al [8] prepared hydrophilic layered silicate/polyurethane nanocomposites via twin screw extrusion and solvent casting. Polyurethane hard microdomains were found to be well-ordered. Tensile strength and elongation were not improved with organosilicate inclusion, Large increases in stiffness were observed. At 7 wt% of organosilicate loading, a 3.2-fold increase in Young's modulus was achieved by solvent casting.

Xu et al [9] showed intercalated poly(urethane urea) (PUU)/organically modified layered silicates (OLS) structures in PUU/OLS nanocomposites. These materials exhibited increased modulus with increasing OLS content, while the strength and ductility were not sacrificed. Water vapor permeability was reduced by about fivefold at the highest OLS contents (6 vol %), as a result of PUU/inorganic composite formation.

Pattanayak et al utilized the unreacted isocyanate groups in the chains of prepolymer and chain extended polymers to tether nanoclay particles [10]. The properties of the resultant materials produced by sequential addition of organically treated silicate particles into both prepolymer and the fully formed polymer chains were studied. As high as 216% increase in tensile strength and 87 % increase in elongation at break were observed with 1-2 wt% of organically treated clay particles.

Most of the previous researches employed nano-sized particles with layered structures, where intercalation or exfoliation could occur during composite synthesizing or compounding. In this study, nano-sized calcium carbonate particulates, without layered structure, were melt-compounded with TPU. Tensile modulus and strength of the TPU/NPCC nanocomposites were studied under different NPCC loadings. Rheological properties under both steady and dynamic shear were reported. The striking influence of fatty acid NPCC coating on the rheological behavior of the composites was examined.

Experimental

Materials

The thermoplastic polyurethane elastomer employed in this study was polyether-based Pellethane 2103-70A from Dow Plastics. Its ultimate tensile strength is 24.7 MPa and ultimate elongation is 730%. Commercial nanosized precipitated calcium carbonate (NPCC) of cubic shape was obtained from NanoMaterials Technology Pte Ltd, Singapore. The primary particle size of NPCC lies between 30 to 50nm. Two kinds of NPCC i.e. NPCC201 and 401 were employed in this study. They differ from each other only in their coatings. According to the manufacturer, NPCC 201 is coated with stearic acid and NPCC 401 is coated with a mixture of fatty acids. The coating method and the composition of the fatty acids mixture are not available from the manufacturer. Fatty acid coatings are employed to decrease the surface energy of the NPCC particles and therefore to promote the dispersion in polymer matrices.

Sample preparation and characterization

Both TPU and NPCC were dried in a vacuum oven at 70°C for 24 hours to remove moisture. A Haake Reocord 90/Rheomex TW100 conical twin screw extruder was employed to homogeneously compound NPCC and TPU. The extruded strand was guided through a water bath to solidify and then granulated by a pelletizer. Compounding temperature was 170^{o}C and screw speed was 100 rpm. TPU/NPCC composites with various NPCC loadings, i.e. 2, 4, 6, 8 and 10 wt % were compounded. The compounding process was run twice for each composite to improve its homogeneity.

NPCC particles were dispersed in ethanol. An ultrasonic bath was employed to break up the NPCC aggregates in ethanol. The suspension was then dripped on a conductive carbon tape. After ethanol evaporation, the carbon tape together with NPCC particles left on its surface was coated with gold for SEM analysis. For TPU/NPCC composites, the samples were fractured in liquid nitrogen. The fracture surfaces were coated and examined. Energy Dispersive X-ray Spectroscopy (EDXS) was also employed to detect the calcium atoms in NPCC.

Thermogravimetric analysis (TGA) was carried out in nitrogen atmosphere at a heating rate of 20 °C/ min on a Perkin-Elmer 7 thermal analysis system to identify the coatings on the NPCC particles.

Tensile properties of the TPU/NPCC nanocomposites were tested with an Instron 5569. Dried TPU/NPCC pellets were compression molded into sheets and then cut into dumbbell shaped tensile test specimens using a specimen cutting press. A pneumatic fixture designed for film and thread tensile specimens was used to hold the

tensile samples in place. 800-grit sandpapers were placed between the fixture and the specimens to prevent slippage. A cross-head speed of 100 mm/min was used to ensure that the samples would break within the maximum tensile displacement of the machine. The thickness of the tensile bar was recorded at three different points and averaged. The gauge length of the tensile sample was also measured at the beginning of each experiment. The width of the tensile specimen was measured as 4.767 mm and was uniform for all the tensile samples. Each test was repeated five times.
Rheological properties of the composites under steady and dynamic shear were studied by a strain-controlled rotational rheometer (ARES from Rheometric Scientific) using parallel plates. All tests were run at 200 ^{o}C. Shear rate ranged from 0.03 ~ 500 s^{-1} in steady shear. In dynamic shear, a strain sweep test was first run to determine the linear viscoelastic region of the composites. Subsequently the viscoelastic properties as a function of shear frequency were studied in the linear viscoelastic region. The frequency ranged from 0.1 to 100 rad/s.

Results and Discussion

NPCC powder and composites morphology

It was difficult to break up the aggregates of nano-sized particles and keep the particles separated due to their high surface tension. Figure 1 (a) shows that NPCC aggregates after ultrasonic dispersion were still as large as 20 microns. This large size was most probably due to the re-agglomeration of separated particles on the carbon tape during the evaporation of ethanol solvent. Under higher magnification, in Figure 1 (b), it was discernable that these aggregates consisted of a large number of smaller aggregates of the size of 100 ~ 200 nm. A micrograph of single particles was not available due to limitation of the sample preparation.

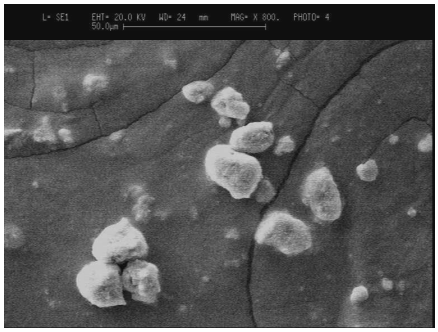

(a) NPCC 401

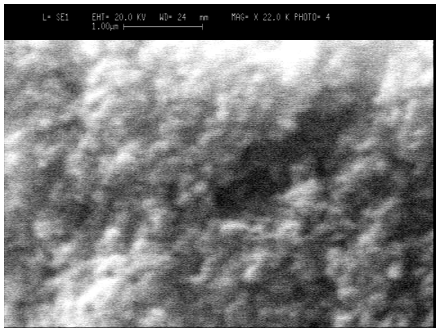

(b) NPCC 201 under high magnification (22K)

Figure 1. SEM micrographs of NPCC particles/agglomerates.

The morphologies of the fracture surface of neat TPU and TPU/NPCC201 composites are shown in Figures 2 (a)-(b). The white round dots in Figure 2 (b) are NPCC agglomerates. This shows that a number of NPCC agglomerates measuring ~ 2 micron still existed in the TPU matrix even after two passes of twin screw mixing. The existence of micron sized NPCC agglomerates in the matrix might limit the property improvement

of the TPU/NPCC composites. The fracture surfaces of TPU/NPCC401 demonstrate very similar morphologies and hence their SEM micrographs are not shown.

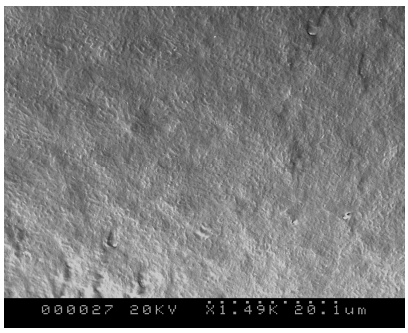

(a) Neat TPU

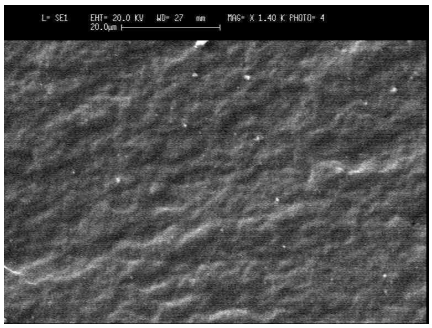

(b) 8% NPCC 201

Figure 2. SEM micrographs of TPU/NPCC composites.

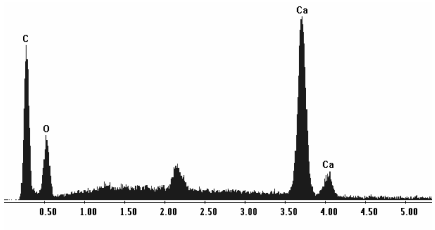

(a) $CaCO_3$

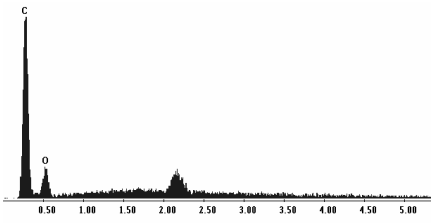

(b) Neat TPU

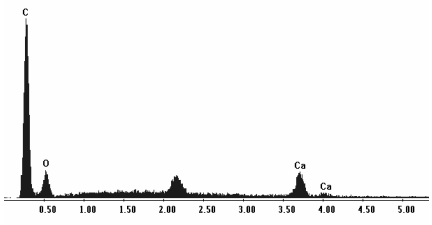

(c) TPU matrix of the composites

Figure 3. EDXS graphs of TPU, NPCC and their composites.

Nano-sized NPCC particles could not be observed in the SEM micrographs due to equipment limitation. However, they might be detected by Energy Dispersive X-ray Spectroscopy (EDXS). The interaction between the energetic monochromatic electrons from an impinging electron beam and the electrons in the atoms of the specimen results in the generation of X-rays. Characteristic X-rays are always of a specific energy or wavelength and identify the elements in a specimen. The electron microprobe instrument utilizes a stationary beam of electrons to excite X-rays from the sample area of interest. The X-rays are characterized by their specific wavelength with an energy dispersive X-ray analyzer (EDXA) attachment to the SEM.

Before running EDXS, the interested area under SEM was enlarged to occupy the whole screen. Figure 3 (a) is the EDXS graph when the focus was on one of the NPCC agglomerates of the TPU/NPCC composites shown in Figure 2 (b). The high calcium peak in the graph indicates the presence of calcium atoms in the agglomerate. When examining pure TPU, no calcium peaks are found, as shown by Figure 3 (b), since calcium atoms do not exist in pure TPU. However, when the SEM was focused on the matrix area (no NPCC particles found by SEM) of Figure 2 (b), traces of calcium atoms are revealed by the EDXS graph (Figure 3 (c)). This indicates that although invisible in SEM, large number of NPCC particles/agglomerates still exist in nano-scale size in the composites.

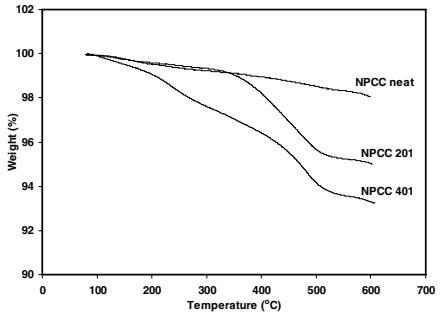

Figure 4. TGA graphs of NPCC particles with different coatings.

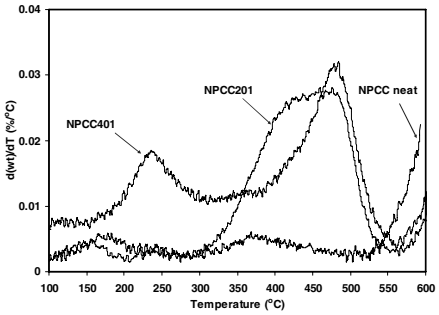

Figure 5. DTG traces of NPCC particles with different coatings.

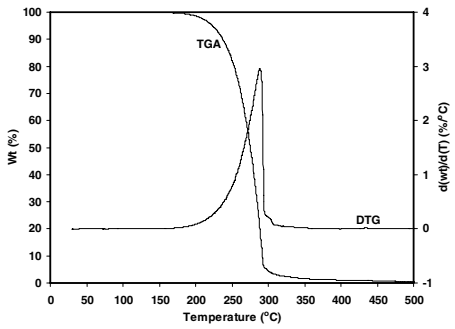

Figure 6. TGA and DTG traces of stearic acid.

Degradation of fatty acid coatings

Figure 4 compares the weight loss of NPCC with different surface conditions. Neat NPCC had a minimal weight loss during the heating process probably due to gradual loss of adsorbed moisture [11-12]. At the same temperature, the weight loss of NPCC401 was always higher than that of 201, indicating more fatty acid coating in NPCC401 than in NPCC201. The decomposition rates of NPCCs in Figure 4 are shown by derivative thermograms (DTG) in Figure 5. Below 500 ^{o}C, the trace for neat NPCC was relatively flat, implying minimal degradation in this temperature range. NPCC201 showed a wide peak ranging from ~400 to ~500 ^{o}C. Since the degradation peak of pure stearic acid was at ~290 ^{o}C, as shown in Figure 6, the wide peak of

NPCC 201 could be due to the degradation of calcium stearate formed on the surface of calcium carbonate particles [12-13]. As for NPCC401, two degradation peaks, locating at ~240 and ~482 ^{o}C respectively, could be observed. Although the composition of the fatty acid coating was unknown, the higher peak was believed to be the decomposition peak of a calcium salt surface layer produced by the reaction of fatty acids and calcium carbonate since no fatty acids had such a high decomposition temperature. The lower peak at ~240 ^{o}C was due to the decomposition of fatty acid itself. Osman et al [12] found three decomposition peaks on excessively stearic acid coated calcium carbonate. The highest peak at ~335 ^{o}C belonged to a monolayer of calcium stearate bicarbonate formed by chemical reaction. One acid molecule reacts with every Ca^{2+} on the surface and the chains are vertically oriented to the surface. In the outer layer the stearic acid molecules are intercalated between chemisorbed molecules. This layer of stearic acid decomposes at ~200 ^{o}C. Excess free acid molecules decompose at ~ 285 ^{o}C, matching the decomposition temperature of pure stearic acid as shown in Figure 6. The free and intercalated acid molecules could be removed from the particle surface by washing with solvent [12]. In light of this, the peak at ~240 ^{o}C in NPCC401 could be due to either intercalated or free fatty acids on the NPCC surface. Either of them could be removed from the particle surface and dissipated into the TPU matrix during the melt compounding process. In contrast, NPCC201 had no excess stearic acid coating and all the acid molecules were chemically bonded to the particle surface. Therefore, they would most likely remain attached to the surface after compounding.

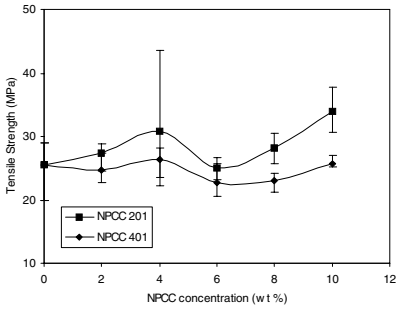

Figure 7. Tensile strength of TPU/NPCC composites with various NPCC concentrations.

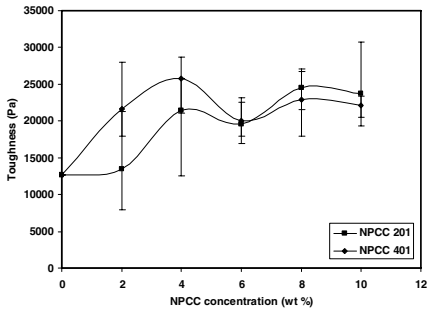

Figure 8. Toughness of TPU/NPCC composites at different NPCC concentrations.

Tensile properties

The tensile strength of TPU shows a moderate increase with the addition of NPCC201, as evidenced in Figure 7. The strength of TPU/NPCC401 was statistically unchanged with increasing loading of NPCC401. Tensile toughness, as measured by the area under the tensile stress-strain curve, demonstrates a more pronounced improvement for both NPCC 201 and 401 composites (Figure 8). These results illustrate that the mechanical performance of TPU was improved with the addition of NPCC 201 and 401. TPU/NPCC401 shows lower tensile strength and higher toughness than TPU/NPCC201. This is most likely due to free fatty acids, which acted as plasticizer in the NPCC401 composites. The property improvement was limited in general, possibly due to the poor dispersion of NPCC in the matrix as revealed by

SEM. Particle agglomeration reduced the surface area of particulates and therefore the interfacial area with the polymer matrix. As such, the overall bonding strength between the particle and matrix was poor. Thus, it is expected that the composites could have higher tensile modulus and toughness should the NPCC be better dispersed. Compared to the mechanical property improvements reported by other researchers [1-10], the improvement in this study is not significant. The major reason is that the particles with layered structures were used in their research. Single layers with large aspect ratios (in the order of 10^2, layer thickness ~1 nm) were dissipated in the polymer matrix when the layered structures were exfoliated. These single layers have much more pronounced reinforcing effects than the cubic NPCC particles with ~30 nm in diameter.

Rheology

Small-amplitude oscillatory shear was conducted within the linear visco-elastic region of the sample. The internal structure of the sample would not be ruptured during the test. The sample was just probed rheologically for its "unperturbed structure". When a macromolecular chain is subjected to a small shear deformation, the chain deforms from the initial spherical shape to an ellipsoid. When the shear is removed, the deformed chain relaxes and recovers its initial equilibrium spherical shape. Polymer melts respond to small-amplitude oscillatory shear through this deformation–relaxation process. At high oscillatory frequencies, the rheological behavior is dominated by the response of the short chains or chain segments that relax quickly. At low frequencies, more time is allowed for relaxation and therefore long chains or complete chains are probed. At very low frequencies, larger scale domains are resonated and phenomena taking place in macro-scale structure such as particle relaxation and particle shape recovery in the case of polymer blends or the relaxation of the whole network in the case of percolating systems can be observed.

Strain sweep tests showed that all materials were in their linear viscoelastic region when the strain was below 10% (figure not shown). Within this region, 5% strain was chosen as the strain for all small-amplitude oscillatory frequency sweep tests. Figure 9 illustrates the variations of G' and G'' of TPU/ NPCC 201 composites with different NPCC 201 loadings. G''s of pure TPU and its composites follow the typical relationship of $G'' \sim \omega$ for polymeric fluids while G's fall below the relationship of $G'' \sim \omega^2$. The variations of G'' were small when NPCC concentration increased from 0 to 10 wt%. The G' and G'' curves exhibit a general trend: the moduli increase with the particle loading, indicating higher flow resistance with more particles. All G'' values are higher than the corresponding G' values, indicating the strong viscous property of the samples within the experimental frequency range. Since the cross over of G' and G'' did not appear yet in the figure, the entire experimental frequency window was within the terminal region of the macromolecular relaxation. At these low frequencies, the response of the whole polymer chains was probed. It is also worth noting that at very low frequencies, plateaus appear on the G' curves with high particle loadings. This solid-like property indicates the existence of NPCC network structures in the TPU matrix [14-16].

In contrast, TPU/NPCC 401 composites demonstrated very different rheological behaviors, as shown in Figure 10. G' increased with NPCC loadings at low frequencies but decreased at high frequencies. G's of all the composites were higher than that of pure TPU at low frequencies and lower than that at high frequencies.

G' curves of all the composites cross the G' curve of pure TPU roughly at the same frequency, i.e. 3 rad/s. In contrast, G'' decreased with NPCC in the whole frequency range and there was no cross over on the G'' curves. G' was very sensitive to microstructures of the sample. G' of the composites was a combined result of the TPU matrix, NPCC fillers and fatty acids coating. The opposite G' behaviors above and below 3 rad/s indicate that two different structures in the composites were probed in the two frequency regions. Below 3 rad/s, resembling TPU/NPCC 201, TPU/NPCC 401 low concentration composites also show solid-like plateaus on G' curves at low frequencies, which implies relatively large scale network structures in the composites. The increasing G' with higher NPCC loading indicates that more NPCC particles caused stronger network structure. With increasing frequency, the dominant response came from the smaller structures, e.g. TPU macromolecules and then free fatty acid molecules within the testing fluid. Fatty acids were immiscible with TPU and had much lower G' and G'' at the testing temperature. During compounding, the intercalated and free fatty acids on the surface of NPCC401 particles were distributed evenly into the TPU matrix and existed as small droplets. Their existence in the composites lowered the modulus of the system at high frequencies where smaller molecules were mostly sampled by the rheometer. Higher NPCC percentage meant more fatty acids in the system, therefore lower G' and G''.

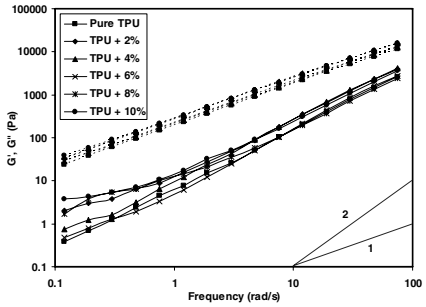

Figure 9. G' and G'' as a function of frequency of TPU/NPCC 201 composites with different NPCC contents (G': solid line, G'': dashed line).

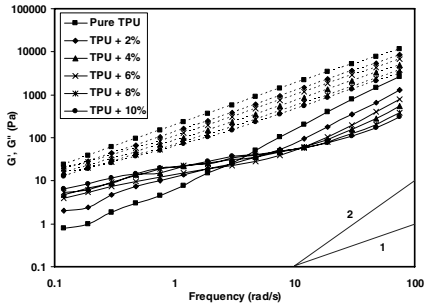

Figure 10. G' and G'' as a function of frequency of TPU/NPCC 401 composites with different NPCC contents (G': solid line, G'': dashed line).

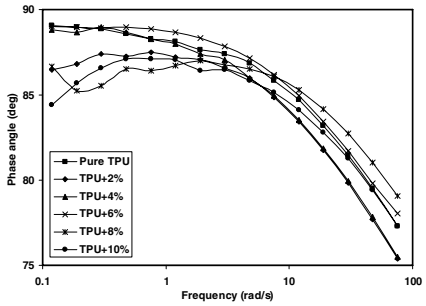

Figure 11. Phase angle as a function of frequency of TPU/NPCC201 composites.

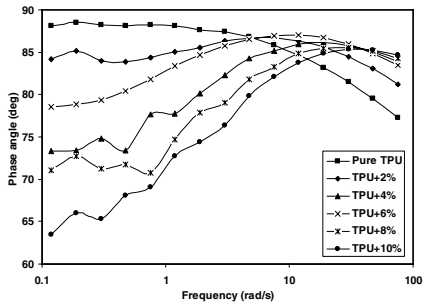

Figure 12. Phase angle as a function of frequency of TPU/NPCC401 composites.

Comparing the phase angles of NPCC201 and 401 composites shows their disparity in rheology property from another aspect. The phase angle of TPU/NPCC201 decreased with dynamic shear frequency, as expected for polymeric fluids (Figure 11). The fluid became more and more elastic with shorter flow characteristic time. However, TPU/NPCC401 showed a very different behavior: increasing phase angle with frequency (Figure 12). Fatty acids were Newtonian fluids at the testing temperature and had phase angles close to 90 degree. With increasing frequency, dissipated fatty acids played a bigger role in the overall rheological behavior of the composites and therefore increased the phase angle of the composites. The phase angle reached a maximum under the competing factors of large phase angle of fatty acids and decreasing phase angle of TPU matrix. The phase angle of the composite adopts the declining trend of the TPU matrix after the frequency passed the maximum-phase-angle frequency. It is also noticed that the phase angle of NPCC401 composite was lower than that of NPCC201 at low frequencies, indicating that NPCC401 composite was more solid-like than NPCC201. This might be due to the complex morphology of TPU/NPCC/fatty acid ternary blend.

TPU/NPCC201 and 401 composites also showed vastly different behavior in steady shear tests. For 201, shear viscosity increased slightly with NPCC loading as shown in Figure 13. The increase in viscosity is a common phenomenon in particle filled polymers since the particles enhance flow resistance. However, the generally observed yield stress and shear thinning behavior at low shear rates due to the destruction of the particulate network structure in filled polymer system was not observed in 201 composites even at highest NPCC loading where dynamic tests demonstrated solid-like structure. This is possibly due to the strain-controlled rheometer employed (a stress-controlled rheometer would be more sensitive in this case) or simply because the shear rates employed were not low enough. For 401 composites, the viscosities of the composites were all lower than that of pure TPU matrix and decrease with increasing particle contents, see Figure 14. This unusual behavior might be explained by the dissipated fatty acids in the TPU matrix, acting as lubricant to lower the viscosity of the composites. Fatty acids, as processing aids, are widely used in polymer industry as internal/external lubricants to reduce the viscosity of polymer melt and the hardness of the final products. Higher NPCC concentration meant more fatty acids in the TPU/NPCC401 composites and therefore lower viscosities. Figure 15 also shows that the 401 composites had two shear thinning stages. The lower one occurred between 0.1 to 4.8 s^{-1} when the NPCC content was equal or higher than 6%. The higher one, occurring at ~100 s^{-1}, was equivalent to the non-Newtonian transition of the pure TPU. Therefore the higher transition should be due to molecular orientation of the TPU matrix. The lower transition is believed to correspond to the structure evolvement of TPU/NPCC particles/fatty acid droplets under shear. The existence of two plateau/shear-thinning regions in the shear rate-viscosity curve is uncommon for particulate filled polymers. Such kind of viscosity behavior has been found in liquid crystalline polymer due to the existence of two levels of structure: molecular and mesoscopic [17]. Similar viscosity curves were also detected in homogenous polymer blends near phase separation temperature and attributed to shear induced homogenization [18] and/or to the existence of two relaxation process in the two-phase region [19]. In our case, fatty acids might migrate to the surface of the parallel plates during rheological tests and caused premature viscosity drop due to wall slip. However, the same viscosity trend was obtained when the serrated parallel plates were employed to prevent wall slip. In addition, Figure 14 also shows that more

NPCC particulates (more fatty acids) caused more pronounced shear thinning behavior. There was no such shear thinning region in NPCC201 composites where all stearic acid molecules were attached to the particulates. Therefore, it is believed that the first shear thinning behavior in NPCC401 composites was caused by the dissipated fatty acid droplets in the TPU matrix. Shear thinning is generally induced by the destruction of higher order structure in the fluid and molecular alignment along flow direction. However, how the fatty acids, NPCC particulates and TPU interacted with each other and caused shear thinning when under shear is not fully understood yet. Further study is required to determine the structural evolvement in the composites under steady shear.

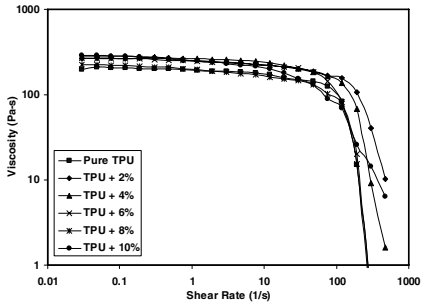

Figure 13. Steady shear viscosities of TPU/NPCC201 composites at various NPCC201 loadings.

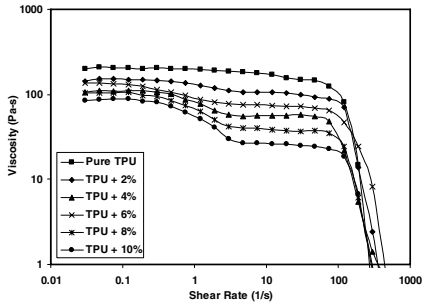

Figure 14. Steady shear viscosities of TPU/NPCC401 composites at various NPCC401 loadings.

Conclusions

Mechanical and rheological properties of TPU/NPCC composites have been investigated. SEM results show that NPCC tends to agglomerate into micron-sized particles. Tensile modulus of the composites increases slightly with NPCC concentration while the toughness increases to a higher degree. The poor dispersion of NPCC may limit the mechanical property improvement.

TPU/NPCC 201 and 401 demonstrate very different rheological behavior in both steady and dynamic shear. TPU/NPCC 201 shows behavior expected for particulate filled polymer, whereas 401 shows quite a unique one. This sharp contrast is believed to be caused by the different status of the fatty acids in the 201 and 401 composites. The free fatty acids in 401 composite induced its unique rheological behavior. The structure evolvement under shear needs to be addressed to explain the behavior.

References

[1] Kojima Y; Fukumori K; Usuki A; Okada A; Kurauchi T（1993）J Mater Sci Lett 12:889
[2] Kojima Y, Usuki A, Kawasumi M, Okada A, Kurauchi T, Kamigaito O (1993) J Appl Polym Sci 49:1259
[3] Kojima Y, Usuki A, Kawasumi M, Okada A, Fukushima Y, Kurauchi T, Kamigaito O (1993) J Mater Res 8:1185
[4] Kojima Y, Usuki A, Kawasumi M, Okada A, Kurauchi T, Kamigaito O (1993) J Polym Sci Part A: Polym Chem 31:983

[5] Tien YI, Wei KH (2001) Polymer 42:3213
[6] Tien YI, Wei KH (2002) J Appl Polym Sci 86:1741
[7] Tortora M, Gorrasi G, Vittoria V, Galli G, Ritrovati S, Chiellini E (2002) Polymer 43:6147
[8] Finnigan B, Martin D, Halley P, Truss R, Campbell K (2004) Polymer 45:2249
[9] Xu RJ, Manias E, Snyder AJ (2003) J Biomed Mater Res Part A 64A:114
[10] Pattanayak A, Jana SC (2003) ANTEC 1424
[11] Keller DS, Luner P (2000) Colloids Surf A 161:401
[12] Osman MA, Suter UW (2002) Chem Mater 14:4408
[13] Fekete E, Pukanszky B, Toth A, Bertoti I (1990) 135(1):200
[14] Zhang Q, Archer LA (2002) 18:10435
[15] Hoffmann B, Dietrich C, Thomann R, Friedrich C, Mulhaupt R (2000) Rapid Commun 21:57
[16] Zhong Y, Wang SQ (2003) J Rheol 47:483
[17] Sigillo I, Grizzuti N (1994) J Rheol 38:589
[18] Takahashi Y, Suzuki H, Nakagawa Y, Noda I (1994) Macromolecules 27:6476
[19] Vlassopoulos D (1996) Rheol Acta 35:556